The interaction of $10^{-3}M$ 1,4-naphthoquinone and F_2 produced new absorbance caused by the corresponding quinol formed upon reduction of 1,4-naphthoquinone by the receptor chemical.

When a sulfhydryl group inhibitor [$10^{-3}M$ *N*-ethyl maleimide (NEM)] was added to either the above mixture or a mixture of the quinone and $10^{-3}M$ reduced glutathione, a change in color occurred upon freezing; however, it was different from that observed in the mixture of quinone and F_2 or glutathione. The known specificity of NEM for sulfhydryl groups would indicate that the naphthoquinones react at sulfhydryl groups on the receptor chemical in F_2 and on reduced glutathione.

In the absence of adequate quantities of purified receptor chemical from F_1 and F_2, complexing between reduced glutathione and 1,4-naphthoquinone, with or without NEM, was further investigated by means of dropping-mercury-electrode polarography. The test solutions were polarographed in 75 ml of deoxygenated 0.1*M* phosphate buffer (*p*H 7.0) and 25 ml of 95 percent ethanol. Changes in the diffusion current of the wave for 1,4-naphthoquinone (Fig. 2) when mixed with reduced glutathione, compared to when analyzed alone, indicated that complexing of these chemicals occurred. In the presence of glutathione, an anodic wave for 1,4-naphthoquinone appeared (Fig. 2), whereas the quinone alone yielded only a cathodic wave. This indicated that 1,4-naphthoquinone had been reduced during its interaction with the glutathione. Upon addition of NEM to the mixture of 1,4-naphthoquinone and glutathione, the diffusion current for the 1,4-naphthoquinone wave fell between that obtained when the quinone was alone and that when it was combined with just glutathione. This would indicate that the addition of NEM reduced the amount of 1,4-naphthoquinone which was complexed with the glutathione. Thus, there was competition between 1,4-naphthoquinone and NEM for sulfhydryl groups on the reduced glutathione.

The findings from our various evaluations of the several naphthoquinones would support the hypothesis that their type of reaction with sulfhydryl groups of F_1 and F_2 is involved in the transduction of energy between the quinone and the sensory neuron. Our findings reveal a naturally operative mechanism for changing the conformation of a receptor macromolecule in nerve membrane. Farah *et al.* (*8*) presented evidence that such a change in conformation of macromolecules in membranes results in an altered flow of inorganic ions through the membrane; and Cole (*9*) discussed the evidence that such altered ion flow may lead to the generation of the electrical potential necessary to fire the neuron.

DALE M. NORRIS
STEPHEN M. FERKOVICH
JACK M. ROZENTAL
JAMES E. BAKER
Deparment of Entomology, University of Wisconsin, Madison 53706

THOMAS K. BORG
Division of Natural Sciences, North Dakota State University, Fargo 58102

References and Notes

1. B. L. Gilbert, J. E. Baker, D. M. Norris, *J. Insect Physiol.* **13**, 1453 (1967); B. L. Gilbert and D. M. Norris, *ibid.* **14**, 1063 (1968); D. M. Norris, *Ann. Entomol. Soc. Amer.* **63**, 476 (1970).
2. D. M. Norris, *Nature* **222**, 1263 (1969).
3. ———, S. M. Ferkovich, J. E. Baker, J. M. Rozental, T. K. Borg, *J. Insect Physiol.*, in press.
4. M. Morrison, W. Steel, D. J. Danner, *Arch. Biochem. Biophys.* **134**, 515 (1969).
5. J. L. Webb, *Enzymes and Metabolic Inhibitors* (Academic Press, New York, 1966), vol. 3.
6. A. Szent-Györgyi, *Bioelectronics* (Academic Press, New York, 1968); *Introduction to a Submolecular Biology* (Academic Press, New York, 1960).
7. T. K. Borg and D. M. Norris, in preparation.
8. A. Farah, N. D. Yamodis, N. Pessah, *J. Pharmacol. Exp. Ther.* **170**, 132 (1969).
9. K. S. Cole, *Membranes, Ions and Impulses* (Univ. of California Press, Berkeley, 1968).
10. Approved for publication by the director of the Research Division, College of Agricultural and Life Sciences. Supported in part by research grants GB-6580 and GB-8756 from the National Science Foundation.

24 July 1970

Slow Synaptic Excitation in Sympathetic Ganglion Cells: Evidence for Synaptic Inactivation of Potassium Conductance

Abstract. *The slow excitatory postsynaptic potential (EPSP) was investigated in frog sympathetic ganglion cells. In contrast to the increased conductance associated with other known EPSP's, during the slow EPSP resting membrane conductance was decreased. Electrical depolarization of the membrane potentiated the slow EPSP, whereas progressive hyperpolarization decreased its size and then reversed it to a hyperpolarizing potential (the opposite of the effect of membrane polarization on other EPSP's). The reversal potential of the slow EPSP was close to the potassium equilibrium potential. We propose that the slow EPSP, in contrast to classical EPSP's, is generated by an inactivation of resting potassium conductance.*

Synaptic excitation results from an increased ion conductance of postsynaptic membrane at virtually all chemically transmitting junctions that have been investigated (*1*). During such typical excitatory postsynaptic potentials (EPSP's), membrane resistance is decreased. The equilibrium potential for the increased ion conductances involved is in the depolarizing direction so that electrical hyperpolarization of the membrane increases the EPSP, whereas progressive depolarization decreases and then reverses the EPSP to a hyperpolarizing potential. The slow EPSP of frog sympathetic ganglion cells has recently been reported to differ from typical EPSP's in that the membrane resistance is increased during the slow EPSP and hyperpolarizing current reverses the slow EPSP to a hyperpolarizing potential (*2*). We have investigated the mechanism of this slow synaptic excitation; we now report evidence consistent with the hypothesis that the slow EPSP is generated by a decrease of resting potassium conductance.

The tenth lumbar sympathetic ganglion of the bullfrog (*Rana catesbeiana*) was studied in vitro with continuous perfusion of oxygenated Ringer solution (*3*). Intracellular records were taken from sympathetic ganglion cells with 15- to 25-megohm microelectrodes filled with 3*M* KCl. Standard techniques of electrophysiological recording were used, current being injected through the recording microelectrode by means of a Wheatstone bridge (*4*). Preganglionic B fibers were stimulated in the sympathetic chain between the sixth and seventh ganglia (*5*). Type B ganglion cells were identified on the basis of antidromic conduction velocity (*6*).

The fast EPSP in frog sympathetic ganglion cells, like most EPSP's, is due to increased ion conductance (*7–9*). Hyperpolarization of the membrane increases the fast EPSP, and depolarization decreases its size (Fig. 1A); fur-

ther depolarization then reverses the fast EPSP to a hyperpolarizing potential. When this fast EPSP is blocked by addition of nicotine (5 μg/ml) to the bath, repetitive stimulation of B fibers generates a slow depolarization in type B ganglion cells (Fig. 1B, part 1)—the muscarinic slow EPSP. (*5, 7, 10*).

The membrane resistance, measured by a constant current pulse, increases significantly during the slow EPSP (Fig. 1B, part 2; *11*), confirming previous observations (*2*). Since electrical conductance is defined as the reciprocal of resistance (*12*), this increase in resistance during the slow EPSP may be considered a decrease in membrane conductance.

We investigated the mechanism of decreased conductance during the slow EPSP by electrical polarization of the ganglion cell membrane. Contrary to the effect on the fast EPSP, depolarizing current increased the size of the slow EPSP (Fig. 1C), whereas hyperpolarizing current decreased the slow EPSP. Further hyperpolarization of the membrane reversed the slow EPSP to a hyperpolarizing potential (Fig. 1C, two bottom records). The relationship of the size of the slow EPSP to polarizing current is shown in Fig. 1E; the size of the slow EPSP was inversely related to membrane potential (*13*). The reversal potential for the slow EPSP occurred at a membrane potential of approximately — 88 mv (*14*). This potential is near the estimated potassium equilibrium potential for vertebrate nerve cells (*1, 15*). A better index of the K^+ equilibrium potential is the reversal potential of the after-hyperpolarization of the antidromic spike (*1, 16*). As shown in Fig. 1D, the after-hyperpolarization of the cell illustrated in Fig. 1, B to E, also reversed at a membrane potential near — 88 mv (*17*). The reversal potential of the after-hyperpolarization is shown in Fig. 1E as an arrow; the reversal potential

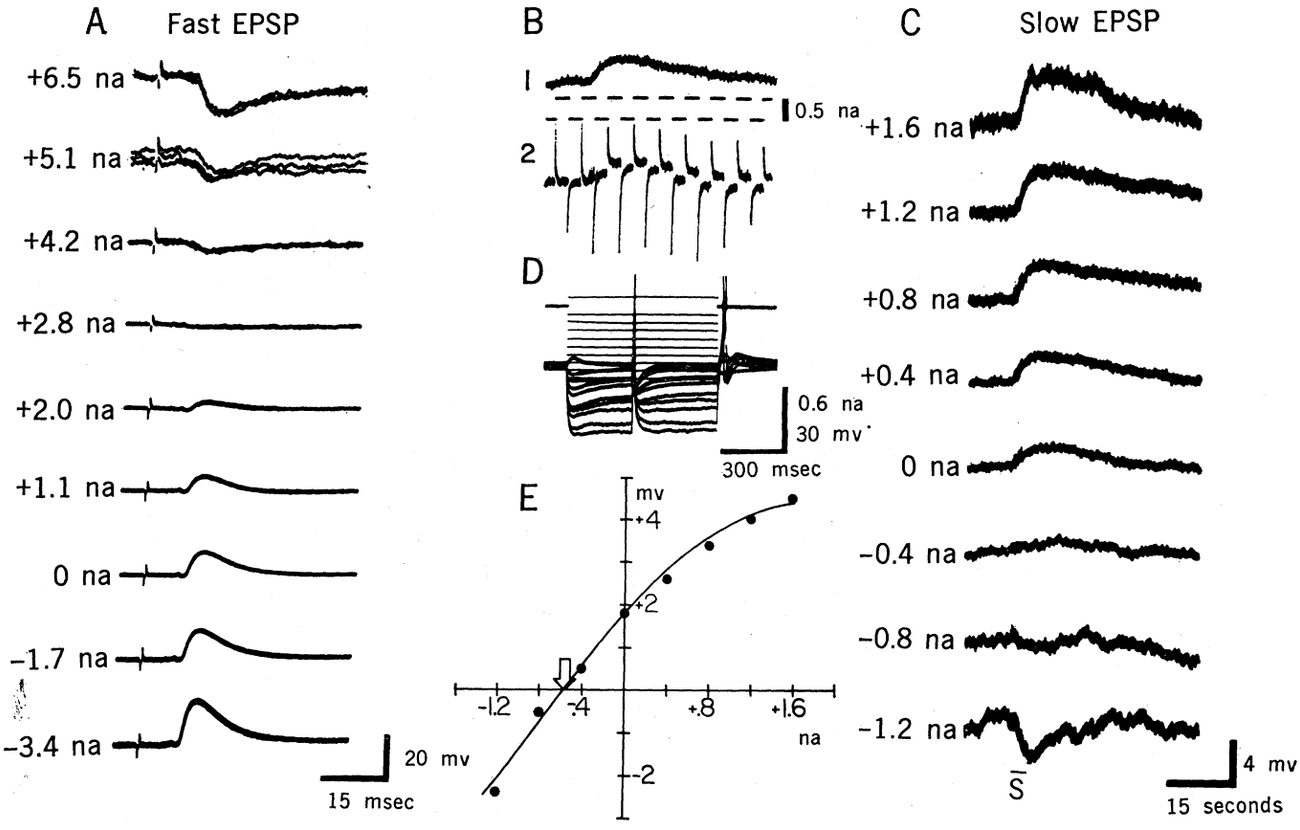

Fig. 1. Fast and slow EPSP's. (A) Amplitude of fast EPSP as a function of depolarizing (+) and hyperpolarizing (—) current. Polarizing current is indicated in nanoamperes. B fibers were stimulated with a single, 0.5-msec stimulus to generate the fast EPSP in a type B ganglion cell. (B and C) Slow EPSP in a type B ganglion cell. The cell recorded stably for over 6 hours. Resting membrane potential was —65 mv; input membrane resistance was 48 megohms. The fast EPSP was blocked by nicotine (5 μg/ml). B fibers were stimulated repetitively at a frequency of 100 per second for 2 seconds. Stimulation began 10 seconds after the beginning of each record. Most of stimulus artifact was lost in photographic reproduction. The period of stimulation is indicated by a line labeled *S* under the bottom record in C. (B1) Slow EPSP at resting membrane potential. (B2) Upper record: hyperpolarizing constant current pulses of —0.5 na. Lower record: bridge balanced before stimulation such that current pulses produced no voltage deflection. Note that during EPSP the —0.5-na current pulses produced a hyperpolarizing voltage deflection of 1 mv, indicating that the membrane resistance had increased by 2 megohms. Time and voltage calibration for B is the same as for C. (C) Amplitude of slow EPSP in B as a function of depolarizing (+) and hyperpolarizing (—) current. Note that the slow EPSP reversed with hyperpolarizing current, the opposite of fast EPSP in A. (D) Amplitude of antidromic spike after-hyperpolarization as a function of membrane potential. The same cell as B and C. Upper record monitors current; note that the larger hyperpolarizing current traces are superimposed on voltage records. Lower record shows antidromic spike superimposed at various levels of membrane potential. Top of spike was cut off by limitation of oscilloscope excursion. Note that the after-hyperpolarization reverses with hyperpolarizing current between —0.5 na and —0.6 na (*17*). (E) Graphic relationship of amplitude of slow EPSP (in C) to current. The reversal potential of slow EPSP is the point at which the curve crosses the abscissa. Arrow indicates the reversal potential of antidromic spike after-hyperpolarization shown in D. Note that the reversal potential of after-hyperpolarization (arrow) coincides with the reversal potential of slow EPSP (curve intercept).

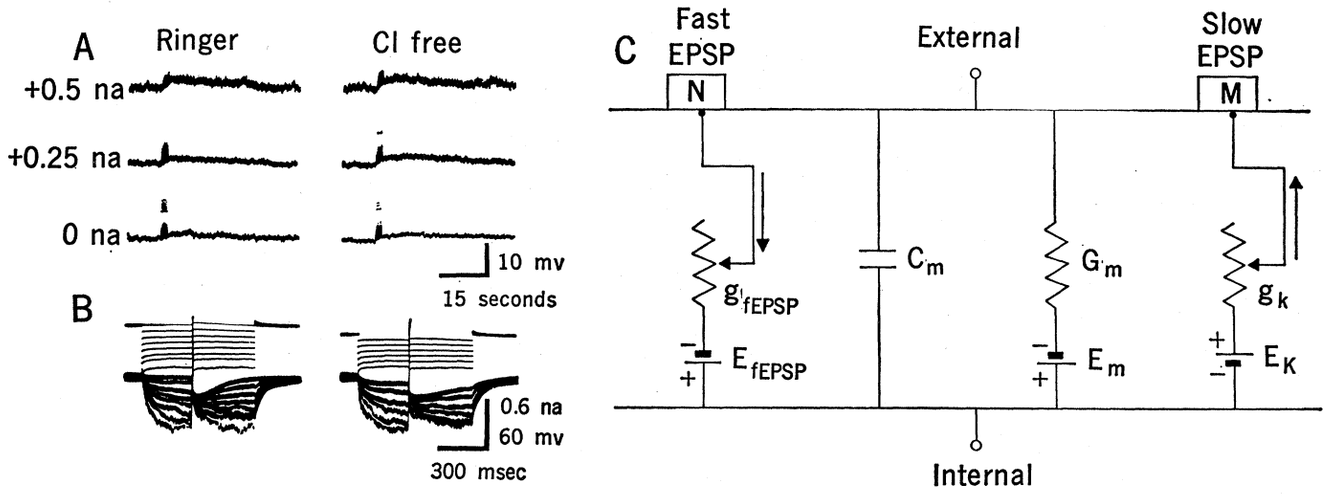

Fig. 2. (A) Effect of removing extracellular Cl^- on slow EPSP. (Left) Potentiation of small slow EPSP by depolarizing current. (Right) Effect of removing extracellular Cl^- on potentiation of slow EPSP by depolarizing current. (B) Effect of removing extracellular Cl^- on reversal of antidromic spike after-hyperpolarization. (Left) Upper record monitors current; lower record shows antidromic spike superimposed at various levels of membrane potential. (Right) Similar to left but after removal of extracellular Cl^-. Note that data taken when Cl^- was removed were recorded over a more limited current range than were control data. (C) Schematic electrical circuit diagram of sympathetic ganglion cell membrane representing the fast EPSP (left) and the slow EPSP (right); C_m represents membrane capacitance. See text for further discussion.

of the slow EPSP and the reversal potential of the after-hyperpolarization are extremely close, if not identical. The similar reversal potential for the slow EPSP and the after-hyperpolarization, taken together with the effect of membrane polarization and the decrease in membrane conductance, strongly suggests that the membrane conductance that is decreased during the slow EPSP is the resting K^+ conductance.

Since the resting conductance and intracellular concentration of chloride ions in sympathetic ganglion cells is not known, the above data do not exclude the possibility of an inactivation of Cl^- conductance. However, the fact that removal of extracellular Cl^- from the Ringer bath (*18*) had no significant effect on the slow EPSP (Fig. 2A) excludes the possibility that an inactivation of a Cl^- conductance plays a significant role in the generation of the slow EPSP. Removal of Cl^- also did not significantly affect the reversal potential of the antidromic spike after-hyperpolarization (Fig. 2B). Inactivation of a resting Na^+ conductance need not be considered for generating the slow EPSP since it would produce a hyperpolarizing response (*19*).

The preceding results are best explained by the hypothesis that the slow EPSP in frog sympathetic ganglion cells is generated by a decrease or inactivation of resting K^+ conductance. The properties of the slow EPSP are explained in terms of this hypothesis as follows. The resting membrane potential is maintained in part by a resting net passive K^+ efflux (*15, 20*). Synaptic inactivation of the resting K^+ conductance would increase the membrane resistance and shift the membrane potential away from the K^+ equilibrium potential and toward the equilibrium potential of the other resting conductances (*21*) resulting in a depolarization—the slow EPSP. Electrical depolarization of the membrane increases the electrochemical gradient for K^+ which increases the passive K^+ efflux; synaptic inactivation of this greater K^+ efflux would generate a larger slow EPSP. Electrical hyperpolarization, on the other hand, decreases the electrochemical K^+ gradient which would decrease the size of the EPSP. At the K^+ equilibrium potential, there is no net passive K^+ flux and no EPSP would be observed. If the membrane is hyperpolarized below the K^+ equilibrium potential the electrochemical gradient for K^+ is reversed, producing a net passive K^+ influx. In this case, inactivation of the K^+ influx would result in a hyperpolarizing potential.

This mechanism may be represented schematically by an electrical circuit diagram of the sympathetic ganglion cell membrane. On the left of Fig. 2C the common type of synaptic conductance mechanism, in this case the fast EPSP, is represented as a variable resistance (the fast EPSP conductance—g_{fEPSP}) in series with an electromotive force (the equilibrium potential for the fast EPSP—E_{fEPSP}) (*22*). Activation of nicotinic membrane receptors (N) is shown increasing the fast EPSP conductance (arrow) which shifts the membrane potential toward E_{fEPSP}. On the right, the slow EPSP mechanism is illustrated as a variable K^+ conductance (g_K) in series with its electromotive force, E_K. In parallel, the other resting membrane conductances are shown as a fixed conductance, G_m, in series with the electromotive force of those resting conductances, E_m (*23*). Activation of muscarinic membrane receptors (M) is illustrated as decreasing g_K (arrow). This would increase the membrane resistance and shift the membrane potential away from E_K and toward the equilibrium potential of the other membrane conductances (E_m), thus generating the slow EPSP.

Inactivation of membrane conductance in several bioelectric tissues has been reported. Depolarizing current inactivates K^+ conductance in eel (*24*) and gymnotid (*25*) electroplaques, whereas strong hyperpolarizing current inactivates K^+ conductance in lobster muscle fibers (*26*) and gymnotid electroplaques (*25*). The response of vertebrate cone photoreceptors to light is a hyperpolarization generated by a decrease in membrane conductance (presumably Na^+) (*19*). Synaptic potentials, on the other hand, result from an increased membrane conductance at virtually all chemically

transmitting junctions that have been investigated (*1*). The slow EPSP in frog sympathetic ganglion cells thus appears to be the first example of a postsynaptic potential generated by an inactivation of membrane conductance. It has recently been reported that acetylcholine acting on muscarinic receptors causes a depolarization of cortical neurons that is not associated with an increased membrane conductance (*27*), and norepinephrine causes a hyperpolarization of cerebellar Purkinje cells that is associated with an increase in membrane resistance (*28*). Although the mechanism of such phenomena needs further elucidation, the similarity of those responses to the slow EPSP in sympathetic ganglion cells suggests that synaptic inactivation of membrane conductance may be a mechanism of general significance in the regulation of neuronal activity.

FORREST F. WEIGHT
JIRI VOTAVA*
Laboratory of Neuropharmacology, National Institute of Mental Health, St. Elizabeths Hospital, Washington, D.C. 20032

References and Notes

1. J. C. Eccles, *The Physiology of Synapses* (Academic Press, New York, 1964).
2. H. Kobayashi and B. Libet, *J. Physiol.* **208**, 353 (1970).
3. The composition of the Ringer solution was: NaCl, 114 mmole/liter; KCl, 2 mmole/liter; $CaCl_2$, 1.8 mmole/liter; $NaHCO_3$, 2 mmole/liter; and glucose, 1 g/liter.
4. T. Araki and T. Otani, *J. Neurophysiol.* **18**, 472 1955); A. R. Martin and G. Pilar, *J. Physiol.* **168**, 443 (1963).
5. B. Libet, S. Chichibu, T. Tosaka, *J. Neurophysiol.* **31**, 383 (1968).
6. S. Nishi, H. Soeda, K. Koketsu, *J. Cell. Comp. Physiol.* **66**, 19 (1965).
7. K. Koketsu, *Fed. Proc.* **28**, 101 (1969).
8. S. Nishi and K. Koketsu, *J. Cell Comp. Physiol.* **55**, 15 (1960).
9. H. Kobayashi and B. Libet, *Proc. Nat. Acad. Sci. U.S.* **60**, 1304 (1968).
10. S. Nishi and K. Koketsu, *J. Neurophysiol.* **30**, 109 (1968); T. Tosaka, S. Chichibu, B. Libet, *ibid.* **31**, 396 1968).
11. In Fig. 1B, part 2, the bridge had been previously balanced in such a way that the hyperpolarizing current pulses did not produce a voltage deflection. This method indicates any change in membrane resistance (ΔR). During the slow EPSP, the —0.5 na hyperpolarizing current pulses produced a hyperpolarizing voltage deflection of 1 mv, indicating that the input membrane resistance had increased by 2 megohms. This increase in resistance was consistently observed and lasted for the duration of the slow EPSP. In this cell, the slow EPSP lasted for 50 seconds beyond the end of the oscilloscope sweep shown; during this time the resistance returned to the level before stimulation. In other experiments, without nicotine blockade, we have found [F. Weight and J. Votava, *Pharmacologist* **12**, 225 (1970)] that after repetitive stimulation of B fibers the mechanism of increased conductance of the fast EPSP lasts many seconds. In this cell, the increased resistance was not maximum during the early part of the slow EPSP, presumably because the fast EPSP (with increased conductance) was not totally blocked by nicotine. In other cells, however, the peak of the increased resistance occurred at the peak of the slow EPSP.
12. A. L. Hodgkin and A. F. Huxley, *J. Physiol.* **117**, 500 (1952).
13. With hyperpolarizing current the current-voltage relationship of the ganglion cell membrane is approximately linear (*8*); however, with depolarizing current we have found that most bullfrog ganglion cells have an increased membrane conductance (delayed rectification). Figure 1E shows that the size of the slow EPSP was approximately linearly related to hyperpolarizing current. Presumably, the falloff in size of the slow EPSP from a linear slope with increasing depolarizing current is due to delayed rectification.
14. In Fig. 1E, the slow EPSP reversed with a hyperpolarizing current of —0.55 na. From the current-voltage relationship of Fig. 1D it can be seen that a current of —0.55 na produced a voltage deflection of approximately —23 mv below resting membrane potential. Since the resting potential of this cell was —65 mv, the reversal potential of the slow EPSP was approximately —88 mv.
15. B. Katz, *Nerve, Muscle and Synapse* (McGraw-Hill, New York, 1966).
16. A. L. Hodgkin and B. Katz, *J. Physiol.* **108**, 37 (1949); B. Frankenhaeuser and A. L. Hodgkin, *ibid.* **131**, 341 (1956); D. A. Baylor and J. G. Nicholls, *ibid.* **203**, 555 (1969). Evidence that the after-hyperpolarization in frog sympathetic ganglion cells is a result of increased K^+ conductance is based on our observations (unpublished) that the amplitude of the after-hyperpolarization was sensitive to changes in extracellular K^+ concentration (being increased by 0 m*M* K_o^+ and decreased by 5 m*M* K_o^+) and that the reversal potential of the after-hyperpolarization was not significantly affected by removal of extracellular Cl^- (Fig. 2B).
17. In Fig. 1D, the after-hyperpolarization reversed with hyperpolarizing currents between —0.5 na and —0.6 na. From the current-voltage relationship in Fig. 1D, the reversal potential of the after-hyperpolarization was near —88 mv (*14*).
18. The composition of the Ringer solution was: Na_2SO_4, 78 mmole/liter; K_2SO_4, 1.6 mmole/liter; $NaHCO_3$, 2 mmole/liter; $CaSO_4$, saturated; and glucose, 1 g/liter.
19. D. A. Baylor and M. G. F. Fuortes, *J. Physiol.* **207**, 77 (1970).
20. A. L. Hodgkin, *Proc. Roy. Soc. London Ser. B* **148**, 1 (1958); *The Conduction of the Nervous Impulse* (Thomas, Springfield, Ill., 1964).
21. In most nerve cells the predominant resting ion conductances are K^+ and Na^+; however, there may also be some leakage conductance ions such as Cl^- (*15*, *20*).
22. The equilibrium potential for the fast EPSP is approximately —10 mv (*6*). There is some evidence that increased Na^+ conductance predominates, but there may also be some increase in K^+ conductance associated with the fast EPSP (*7*).
23. In most membrane circuit diagrams, E_m represents the electromotive force of all resting conductances including E_K. In Fig. 2C, however, E_K is represented separately, and E_m represents the electromotive force for the other resting conductances. Since this would be g_{Na} and leak conductances, E_m is indicated with positive inside and negative outside.
24. F. Ruiz-Manresa, A. Ruarte, T. Schwartz, H. Grundfest, *J. Gen. Physiol.* **55**, 33 (1970).
25. M. V. Bennett and H. Grundfest, *ibid.* **50**, 141 (1966).
26. J. P. Reuben, R. Werman, H. Grundfest, *ibid.* **45**, 243 (1961).
27. K. Krnjević, *Fed. Proc.* **28**, 113 (1969).
28. G. R. Siggins, A. P. Oliver, B. J. Hoffer, F. E. Bloom, *Science*, in press.

* Supported by NIMH international visiting fellowship VF-M1180. Present address: Department of Physiology, Charles University, Prague, Czechoslovakia.

22 July 1970

Predicting Measures of Motor Performance from Multiple Cortical Spike Trains

Abstract. *Recordings have been obtained simultaneously from several, individually selected neurons in the motor cortex of unanesthetized monkey as the animal performed simple arm movements. With the use of comparatively simple quantitative procedures, the activity of small sets of cells was found to be adequate for rather accurate real-time prediction of the time course of various response measurements. In addition, the results suggest that hypotheses concerning the response variables "controlled" by cortical motor systems may well depend upon whether or not the temporal relations between simultaneously active neurons are taken into account.*

The firing patterns of single neurons in the cerebral or cerebellar cortices of unanesthetized animals during the performance of conditioned motor responses have been described in several reports (*1*, *2*). In each of these studies, the basic experimental approach has been the same; recordings have typically been obtained from one cell at a time, and attention has been focused on the extent to which the temporal discharge pattern of a given single unit, or class of sequentially observed units, might convey information concerning the intensity and time course of the animal's movements. Evarts' studies (*2*) of the activity of pyramidal tract (PT) neurons during conditioned hand movements in the monkey provide an excellent example of this type of approach and the kinds of data derived from its use. We now describe a somewhat different approach and present data which suggest that information about a given movement is carried not simply in the discharge patterns or spike trains of individual cortical neurons but to a significant extent by the temporal relations between them.

Our experiments are related to the general question of whether neuronal spike trains might be used for quantitative prediction of simple motor responses (*3*). In particular, we were interested (i) in determining which of the measurements associated with simple arm movements (such as arm